15 (2022) 100192

Contents lists available at ScienceDirect

International Journal of Thermofluids

journal homepage: www.sciencedirect.com/journal/international-journal-of-thermofluids

Analysis of heat transfer and fluid flow in a microchannel heat sink with sidewall dimples and fillet profile

Abdullah K. Okab [a], Hayder M. Hasan [b], Mushtaq Hamzah [c], Karim Egab [b], Ahmed Al-Manea [d,*], Talal Yusaf [e]

[a] Department of petroleum Engineering, University of Thi-qar, Iraq
[b] Department of electromechanical systems engineering, Southern Technical University, Thi-qar Technical College, Iraq
[c] Department of thermal mechanics, Southern Technical University, Basrah Technical College, Iraq
[d] Al-Samawa Technical Institute, Al-Furat Al-Awsat Technical University, Iraq
[e] School of Engineering and Technology, Central Queensland University, Australia

ARTICLE INFO

Keywords:
Microchannel
Fillet profile
Dimples
Heat transfer rate
Friction losses

ABSTRACT

The performance of microchannel with sidewall dimples and fillet profile in the bottom surface is investigated. Two dimple sizes of (0.5 mm and 1 mm) are systematically clustered along the channels with and without fillet are considered. The laminar flow regime is assumed with Reynolds numbers ranging from 200 to 1200. The results show that the dimples and fillet profile have a significant effect on the thermal performance of microchannel. The Nusselt number of the microchannels with 1 mm dimples is 20% higher than the plain microchannel. However, an increase in pressure drop of 10% was obtained. In addition, the fillet profile impacts the thermal performance of microchannels without pressure drop penalty increase. Combining both dimples and fillet profile causes a significant enhancement in the thermal performance. Nusselt number of microchannels heat sink with 1 mm dimple size and fillet profile is 60% higher compared to the plain microchannel.

1. Introduction

Increase deamnd in energy sector motvited reserchers to conduct studies to enhance understanding on the heat transfer in many applications [39,40] .With continuous progress in the enhancement technology methods in the performance of thermal cooling and heat transfer removal, microchannel heat sink devices still play an important role in cooling devices such as thermoelectric devices that are used to cool down the electric chips of computers for example. Various studies have been conducted on the heat transfer improvement in cooling applications to further understand the physical concept of cooling in microchannels [1–13]. Maintaining microelectronic devices within operation temperatures is vital to protect such components. In addition, the applicability of the use of phase change materials makes microchannels an attractive field for researchers. Various techniques were used to improve heat transfer characteristics and to reduce the high-pressure drop cost starting from the plain channels to the modified ones like adding a variety of dimples along the channels, fins and so on. However, one of the major issues that may impact their applications are the high axial heat transferred due to the large channel walls in comparison with their hydraulic diameters [14,15]. Using a MC with an embedded fins structure inside the microchannels enhances the thermal performance due to enhancing the turbulent flow inside the channels. Also, perforation increases the heat transfer area and heat dissipation from the surface and boosts cooling performance [16]. When compared to the plate-fin MC, the enhanced designs' thermal resistance was reduced by 30% at various fluid velocities. A perforated MC increases the heat transfer performance in comparison to the plain MC with the addition of pressure losses [17]. The heat transfer is enhanced due to the increase in the conventional area. Increasing the perforation diameter increased the heat transfer performance while a notice of the pressure drop was increased. The thermal performance of MC that is air-cooled and MC that is air-cooled with perforations in power electronic applications is discussed [18]. The perforated MC can keep the electronic devices in the temperature criteria since it dissipates more heat than the air MC. Surface MC's thermal performance has been improved as a result of the changes in flow behaviour and heat transfer area. The use of knurling on the channel surface improves the heat transmission performance of microchannels [19]. The enhancement of heat transfer of Nu was 255% compared to the smooth surface due to an increase in surface roughness. The roughness causes the separation of the boundary layers and fluid

* Corresponding author.
E-mail address: dr.ahmed.almanea@atu.edu.iq (A. Al-Manea).

https://doi.org/10.1016/j.ijft.2022.100192
Received 28 April 2022; Received in revised form 5 August 2022; Accepted 5 August 2022
Available online 8 August 2022

Nomenclature

L	The microchannel's length (mm)
W	The microchannel's width (mm)
W_l	The single channel's width(mm)
H	The height of microchannel (mm)
H_b	The microchannel base height (mm)
v	Fluid velocity (m/s)
Cp	Specific heat (KJ/kg. K)
k	Fluid thermal conductivity of the (W/m. K)
Nu	Nusselt number
T_f	Fluid temperature (K)
k_s	Solid thermal conductivity of (W/m. K)
T_s	Surface temperature (K)
P	Pressure (pa)
Re	Reynold number
D_h	Hydraulic diameter (mm)
U	overall velocity (m/s)
Q_{eff}	Effective heat transfer rate (W)
Greek symbols	
Δ	Difference
ρ	Fluid density (kg/m3)
μ	Fluid dynamic viscosity (Pa s)
Subscripts	
f	Fluid
in	Inlet
s	Solid

mixing. Moreover, the performance of heat transfers in microchannels improved using the hybrid wettability bottom surface of elliptical patterns [20]. The surface wettability is controlled using sandblasted and smooth surfaces. The heat transfer increased using hybrid patterns and fully sandblasted surfaces compared to the smooth surface.

Modifying the channel geometry at different mass fluxes resulted in a further increase in heat flux in microchannels during flow boiling. The thermal and hydraulic performance of microchannels during flow boiling with various inlet restrictor configurations is investigated. [21]. The intake restrictors improve heat transfer performance at high Reynolds numbers while reducing performance at low flow rates. The restrictors produce high-pressure drop as a penalty of heat transfer enhancement. Heat transfer enhancement of flow boiling in parallel microchannels with interconnecting slots beginning from the middle to the end of the channel is obtained [22]. When compared to plain microchannels, the heat transfer rate is boosted by 172%t due to the mass flux of 462 kg/m^2. Enhanced flow boiling heat transfer in microchannels is performed using multiple micronozzles [23]. For improving the mixing effect and thermal performance, micronozzles with mass fluxes varying from (120 to 600) kg/m^2. s was incorporated. Performance of heat transfer and pressure drop in silicon nanowires microchannels at mass flux ranging from 400 to1600 kg/m^2 s was investigated in comparison with plain microchannels [24]. The silicon nanowires microchannel enhanced the heat transfer performance by 400% more than plain microchannels and recused the pressure drop by 70%. The shape and design of the fins have a major impact on the performance of MC. Changing the fin's shape changes the flow behaviour which increases the heat transfer efficiency. The optimization of heat transfers of the heat sink using pin-fin was tackled in [25]. The heat sink performance was determined by the key parameters like thermal resistance and pressure losses because they influence the forced convection flow. A variety of materials were investigated in this work and different parameters affect the thermal and hydraulic performance of the heat sink. The investigation concluded that the elliptical and circular pin-fin geometries are thermally the best in comparison with other shapes. Generally, all types of inserts that cause circulation to the fluid are favourable to improving heat transfer performance as they allow more fluid to be contacted with hot surfaces. The effect of pin-fin shapes and dimension ratios on the thermal performance of MC is studied. The square pin-fin has a better performance at low air velocity compared to other shapes but higher pressure drop which reduces its effectiveness. The streamlined shape has the best performance at different air velocities with a lower pressure drop penalty. A comparison in thermal performance of plate-fin MC and pin-fin MC was investigated during parallel flow conditions [26]. A comparison in thermal performance of plate-fin MC and pin-fin MC was investigated during parallel flow conditions [27]. The pin-fin MC led to lower thermal resistance than the plate-fin MC at the same heat flux and flow rates. The effect of modifying the cross-sectional shape of the fins (rectangular, trapezoidal, and triangle) on the thermal performance of the MC was investigated [28]. The MC with triangle fin cross-section has the best performance compared to the fins cross-section. In addition, different perforation shapes which are (square, triangle and circle) are conducted on triangle fin cross-section for optimizing thermal performance. Triangular perforation advances the heat transfer performance compared to square and circle perforation. Heat transfer and pressure drop analysis of serpentine microchannels in laminar flow was investigated [29]. The thermal resistance and pressure drop losses were reduced at ranges of Reynolds number of (200–1000) which enhanced the thermal performance. To study the effect of the geometry of the pin-fin on thermal performance and friction losses, different pin fin-shaped were configured [30]. The performance enhances with the use of cone pin fin heat sink while Nusselt number with friction losses increase in case using rectangular pin fin heat sink.

Using dimples increases the heat transfer performance with pressure penalty because they cause fluid circulations and mixing which increases the heat transfer area. Enhancement of heat transfer performance of trapezoidal microchannels with lateral slots and dimples located at the end of the channels was studied [31–33]. Flow separation and vortex generation were noticed at different flow velocities. The dimples improve the heat transfer performance by enhancing the Nusselt number by 108.2% compared to the channel without modifications. A new design of microchannels with circular and elliptic ribs and fillet corners on the bottom surface was investigated to improve the thermal performance [34] and [35]. The heat transfer rate and Nusselt number values indicate that an enhancement of (18–21)% was obtained in the case of elliptic ribs with fillet corners with a slight increase in pressure drop. Heat transfer and fluid flow analysis in microchannels with pin-fins and dimples were investigated. The influence of pin-fin diameter, spacing between fins and depth of dimples were discussed to find the optimum design. The heat transfer increases with increasing the pin-fin diameter and decreasing the spacing between the fins at constant dimples depth. However, increasing the depth of dimples reduces the heat transfer performance, especially at low *Re*. Heat transport in a dimpled channel was investigated using *Re* and dimple dimensions. [36]. The size and buoyancy of the dimple have an impact on the Nusselt number. To boost heat transfer performance, different dimples were created on the heat channels to generate a vortex in the working fluid [37]. When compared to a smooth microchannel, the vortexes and dimples improve heat transfer performance by 23.4–59.8% and increase the friction factor by 22.1–54.4%. To improve the thermal performance of turbulent flow, different perforation forms on heat sink channels were used [38]. Perforation shape improves fluid dynamic performance, with triangular perforated fins having the lowest skin friction coefficient value and efficient heat transfer performance compared to other types of

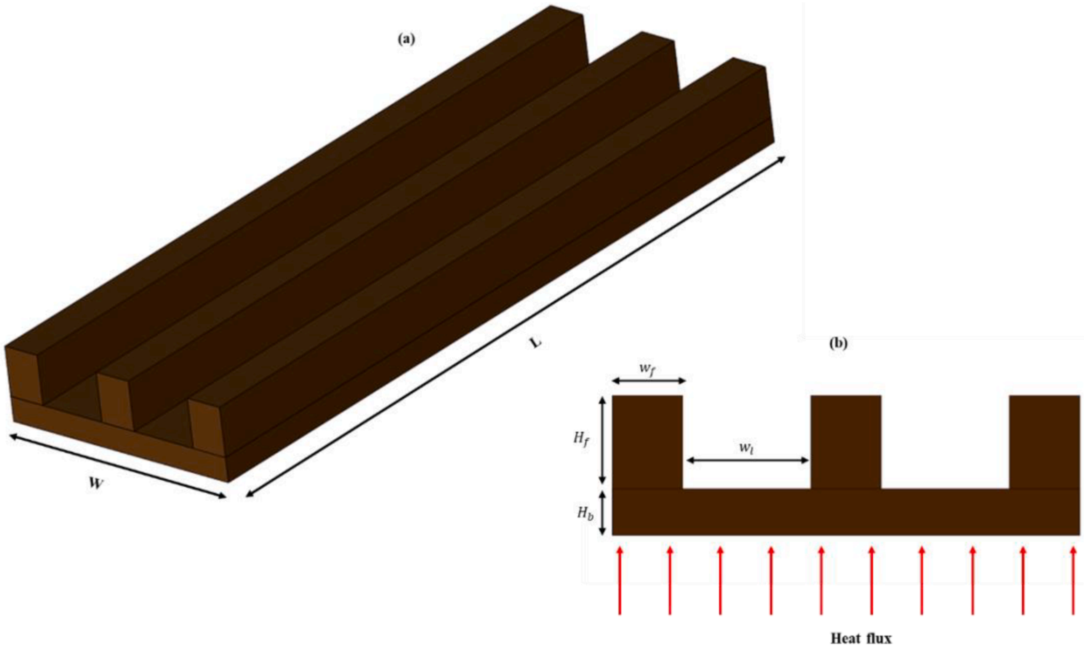

Fig. 1. Microchannels schematic design (a) 3D perspective (b) side view.

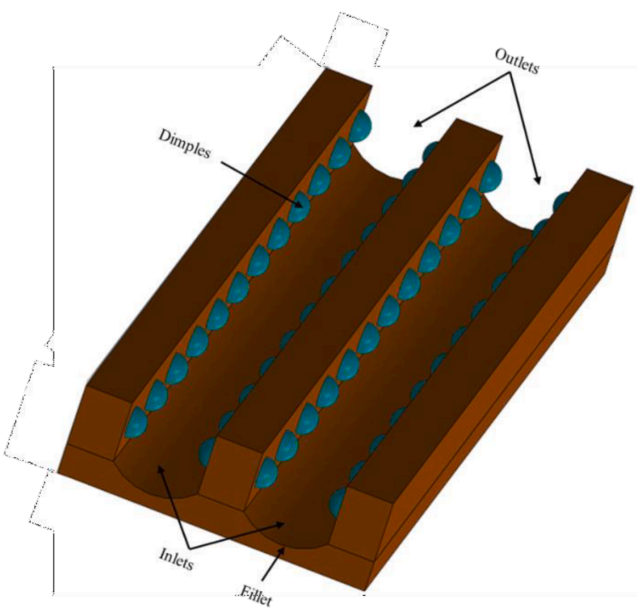

Fig. 2. The microchannels domain, with a fillet profile and a dimple size of 1 mm.

Table 1
The boundary conditions.

Region	Boundarycondition	Expression
Inlet	Velocity	$u = (0.1 - 0.5)$ m/s, $T = 293$ K
Outlet	Pressure	$P = 0$
Bottom wall	Constant heat flux	$-k_s \frac{\partial T_s}{\partial y} = q = 20\ W$ W
Other walls	adiabatic	$\frac{\partial T_s}{\partial y} = 0 = \frac{\partial T_f}{\partial y}$

fins.

To improve the heat transfer rate, improved microchannels with fillet profile and sidewall dimples are proposed in this work. The fillet

Table 2
The thermal properties of aluminium and water.

Material	p	*Cp*	k	μ
Aluminium	2719	871	202.4	
Water	998.2	4181	0.6	0.0010013

Table 3
The grid independence study.

Grid size	Nusseltnumber	Pressure drop Pa
733,888	9.92	28.43
942,784	10.1	28.604
1,136,873	10.15	28.59
1,398,331	10.29	28.68

profile is applied to the bottom channel surface. Two dimple sizes of 0.5 mm and 1 mm forming two rows (one row contains 12 dimples are mounted on each side of the rectangular microchannel) will be conducted. To have a better comparison, the sizes of the same dimples performed on the microchannels with and without fillet will be considered. The fillet configuration refers to that the bottom side of the microchannel is made to be curved downward to boost the amount of the enforced flow. The investigations are applied at different ranges of *Re* under the laminar flow regime. It is not far-fetched in the literature that one of the essential channel flows is dynamics of water regardless of volume. Water is commonly used in the industry because it is readily available, inexpensive, and can dissolve to form a solution, suspension, or colloidal suspension. In view of this, if water is to be used as a heat exchanger, its poor thermal conductivity property characteristics must be changed by incorporating nanoparticles not only because its pH is 7, but could also exist in three states in nature with high surface tension. The dimples cause mixing and circulations in fluid flow while the fillet profile increases the heat transfer area. Investigation of Nusselt number and friction loss effects will be discussed. Studying the thermal of each case's performance is employed to find the optimum enhanced surface.

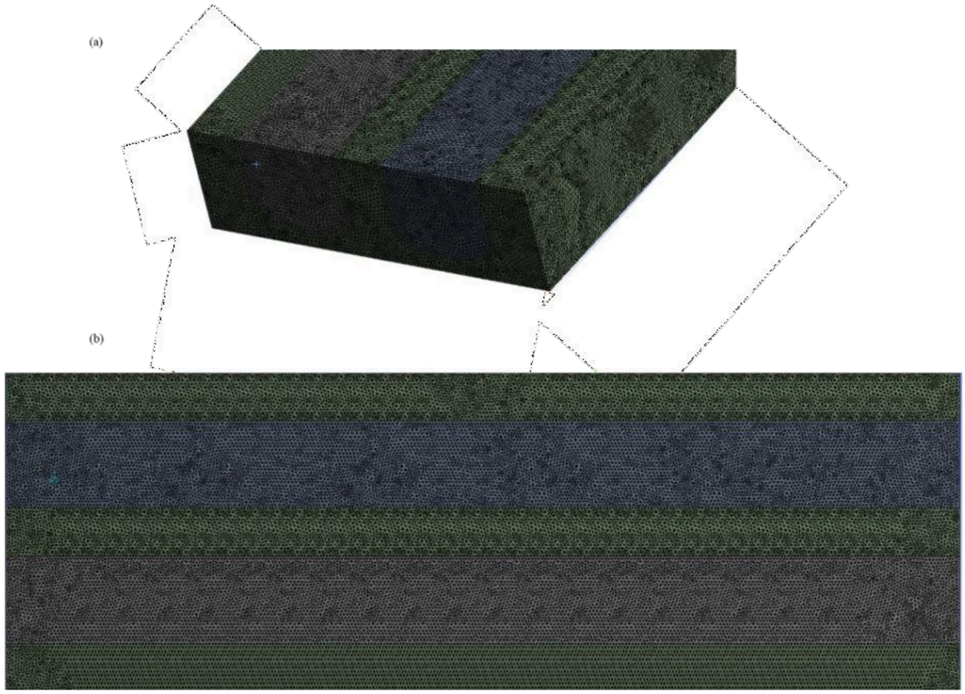

Fig. 3. The mesh and grid for microchannels (a) 3D view (b) top view.

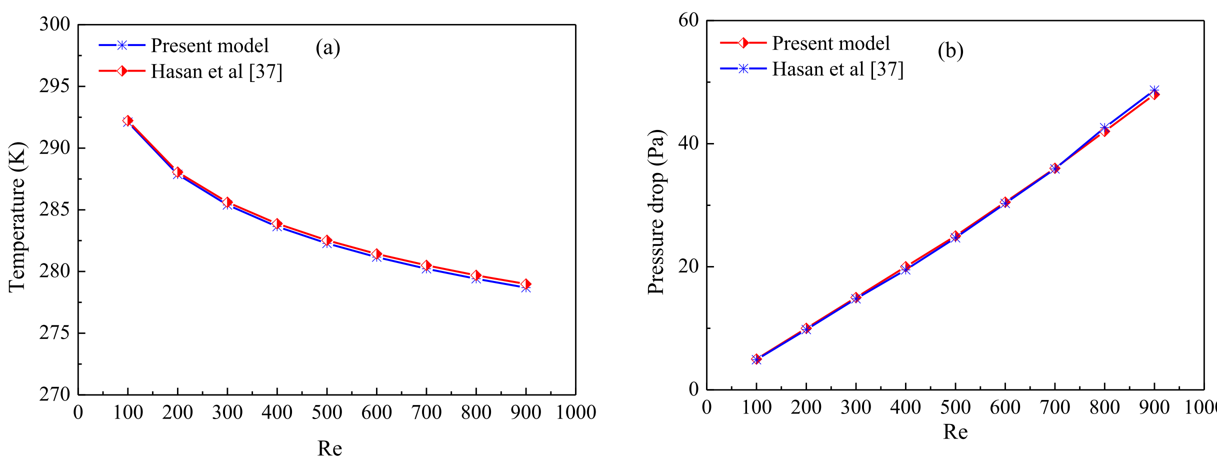

Fig. 4. The comparison results of the present model and [37] results for (a) temperature distribution along the channel and (b) pressure drop.

2. Numerical method and procedure

2.1. Physical model

The schematic design of the microchannels (MC) is shown in Fig. 1. The dimensions of the MC are (L*W) which is (30×10) mm and consists of two channels. The channel width (wl), fin height (Hf), and fin width (wf) are 2.75 mm, 1 mm and 1.5 mm respectively. The Microchannels domain, with a fillet profile, has the same dimension as a flat microchannel with a dimple size of 1 mm. The MC material is aluminium with constant thermo- physical properties. Constant heat flux was applied on the bottom surface of microchannels. To improve the heat transfer performance, a fillet profile was performed on the bottom channel surface and dimples applied on the sidewalls of each fin are designed. The fillet profile depth is 0.5 mm in each channel. The arrangement of dimples was in the horizontal direction with a constant distance between them. The dimples are placed at 1 mm from the entrance of the channel. Microchannels without modification are referred to as MC, microchannels with fillet profiles are referred to as MC-FP, microchannels with dimples are referred to as MC-D, and microchannels with fillet profiles and dimples are referred to as MC-FP-D. Two dimples sizes are investigated of o.5 and 1 mm with both MC-D and MC-FP-D which generates six cases analysed in this work aiming to enhance the thermal performance of microchannels using fillet profile and different dimple sizes along with the plain microchannels. Water is used as a working fluid in all cases. Fig. 2 shows the total domain of the fillet profile MC with a dimple size of 1 mm which is the case (MC-FP-D1.0).

2.2. Governing equations and boundary conditions

The governing equations of fluid flow and heat transfer are Navier stokes equations as follows: Continuity equation:

$$\nabla.\vec{U} = 0 \tag{1}$$

The momentum equation given below in the case of forced convection is considered in this work due to the higher heat transfer rates and

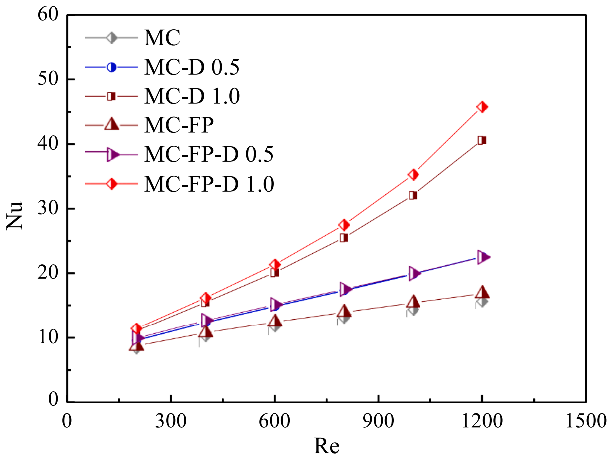

Fig. 5. Variation of the Nusselt number with Reynold number at different configurations of the microchannels.

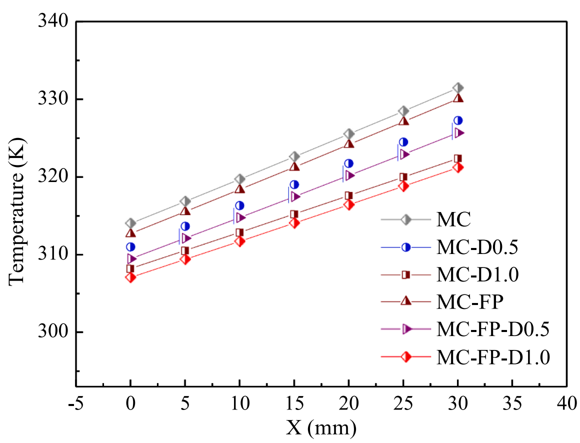

Fig. 6. The temperature distribution along with the MC at $Re = 200$.

more applicable in the complicated systems. Also to allow the flow to overcome the sheer stress that occurs near the channels walls.

$$\rho f\left(\vec{U}.\nabla\vec{U}\right) = -\nabla P + \nabla.\left(\mu_f \nabla\vec{U}\right) \tag{2}$$

Energy equation:

$$\rho_{f.} Cp_f\left(\vec{U}.\nabla T_f\right) = \nabla.\left(k_f \nabla T_f\right) \tag{3}$$

where $\vec{U}$, P, T_f, ρ, C_p, μ and k are velocity, pressure, temperature, density, specific heat, viscosity and thermal conductivity. The subscripts f and s refer to fluid and solid respectively. The thermal calculations in microchannels can be obtained from numerical results. The hydraulic diameter of the channel is defined as:

$$D_h = \frac{4\left(W_1 \times H_f\right)}{2\left(W_1 + H_f\right)} \tag{4}$$

The indicator of the flow regime is conventionally controlled by Reynolds number and it is defined as:

$$R_e = \frac{\rho_f u_i D_h}{\mu_f} \tag{5}$$

The average heat transfer coefficient and Nusselt number is [28]:

$$h = \frac{Q_{ef}}{\left(T_w - T_f\right)} \tag{6}$$

The Nusselt number is:

$$Nu = \frac{h \times D_h}{k_f} \tag{7}$$

The friction losses are:

$$\mathrm{f} = \frac{2\Delta \mathrm{PD_h}}{\rho_\mathrm{f} \mathrm{Lu_m^2}} \tag{8}$$

The boundary conditions are assumed to be uniform for the laminar and steady-state flow inside the channels. Table 1 shows the boundary conditions for microchannels. The water flows in the channel and the MC is made from aluminium. The constant thermal conductivity and dynamic viscosity are considered. The thermal and physical properties of aluminium and water are shown in Table 2.

The thermal performance criteria TPC which is the rate of heat transfer and friction factor for modified and unmodified surfaces is determined on all surfaces. The TPC is defined as [27]:

$$PTC = \frac{(Nu)}{Nu_0} \times \frac{\left(f^{-1}\right)^3}{f_0} \tag{9}$$

The Nu_0 and f_0 were the average Nusselt number and friction factor of the MC without modifications.

2.3. Numerical solution

In this work, the governing equations for solid and liquid domains were solved using the finite volume method with the simulation of Ansys 18.1 software. The geometry was created using Solidwork 2013 software. The velocity, temperature and pressure calculations were simulated with the use of SIMPLEC algorithm. In addition, the continuity, momentum and energy equations were utilized using the second upwind scheme. To obtain the acceptable converging for Navier-stokes equations, the residual for continuity, momentum and energy equations are set to be less than 10^{-6} and 10^{-9} respectively.

2.4. Mesh independence study

A mesh independence study is conducted to ensure that the mesh size does not influence the solution. The dimples and fillet domains are analyzed with finer mesh than other solid and fluid domains to obtain accurate results. An analysis of Nusselt number calculation for case (MC-D-0.5) was achieved to ensure the mesh independence study. The Nusselt number and pressure drop calculations are obtained in Table 3 for different mesh sizes for the case (MC-D 0.5) at $Re = 200$. Therefore, the mesh size of 1,136,873 gives an acceptable accuracy which can be considered in the present study. The 3D view and top view of the mesh and grid for the microchannels are shown in Fig. 3.

3. Model verification

Verification was carried out to validate the numerical solution of the present model by solving and comparing the model design results reported in [37]. The model was consisting of the 3D microchannels with and without different configurations of pin-fins. The length, width and height of the MC are (16, 6 and 1) mm respectively. The pin-fins height and width are 0.5 mm. The working fluid is water with an inlet temperature of 293 K. The calculations were obtained at different ranging of Reynolds numbers between (100–1000) and the bottom surface was exposed to a constant temperature of 373 K. The solution is modelled using the finite volume method, i.e. fluent 18.1 software. Fig. 4 shows the comparison results of the present model and [37] results for temperature distribution along the channel and pressure drop in case of the un-finned MC. The agreement between the present model and [37] is about 3% for temperature and 2% for pressure drop.

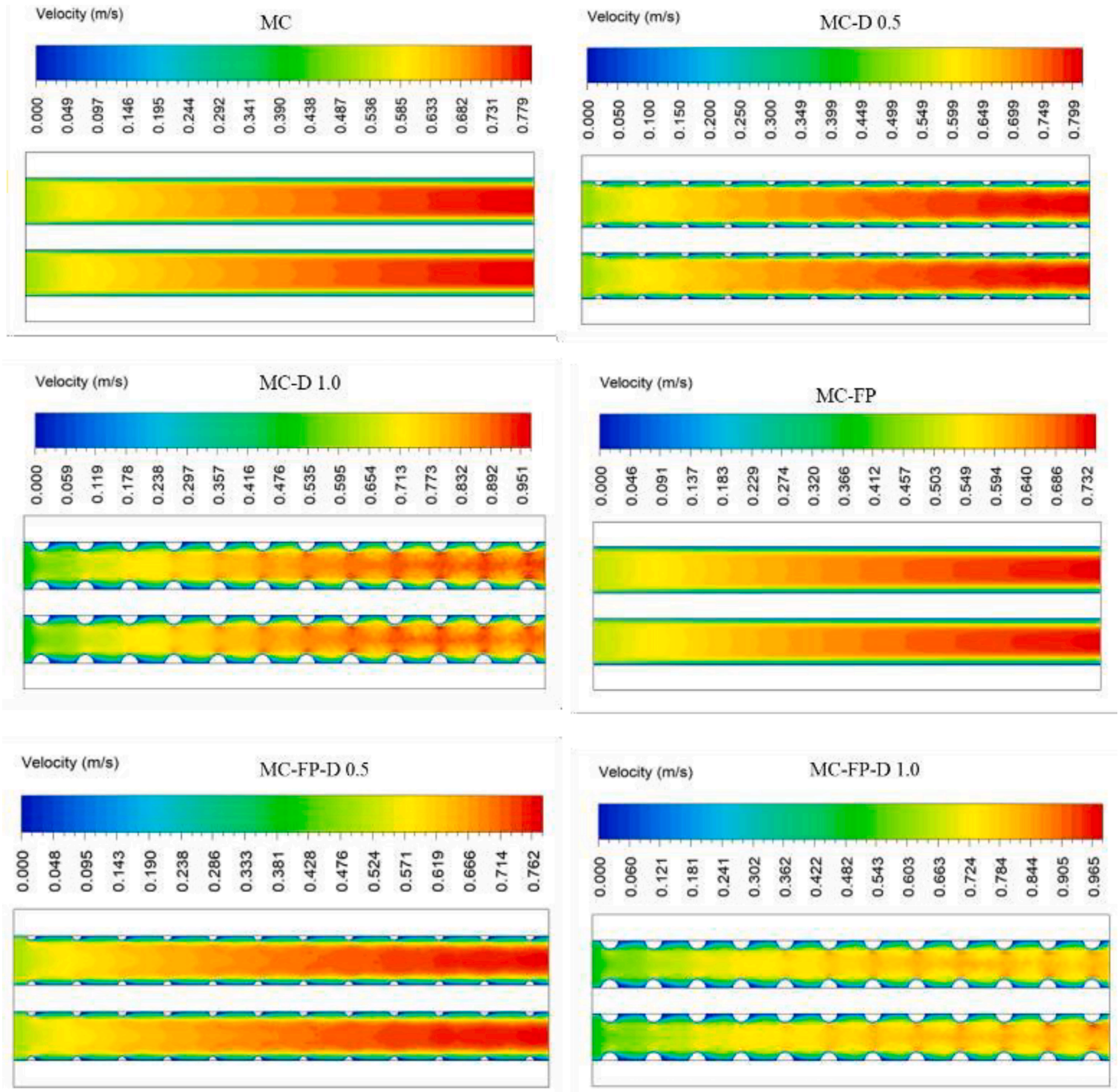

Fig. 7. The velocity distribution behaviours of modified MC surfaces.

4. Results and discussions

4.1. Effect of dimples and fillet profile on thermal performance

To show the influence of fillet profile and dimples on heat transfer in microchannels, various configurations of the (MC) are considered, MC with fillet profile MC-FP, with dimples (MC-D) and with both fillet profile and dimples (MC-FP-D) is performed. Two dimples diameters were investigated 0.5 mm and 1 mm. The same inlets velocity, temperature and heat flux are applied in all case studies (i.e. six cases). The investigation is performed at laminar flow for ranging of Reynolds numbers of (200–1200). The Nusselt number is obtained at different Reynolds numbers as shown in Fig. 5. The heat transfer performance of Nu increases in all cases with increasing *Re*. The performance of fillet profile and fins MC with dimples diameter of 1 mm case MC-FP-D1.0 and MC-D1.0 is the best performance due to the high fluid circulation inside the channels which enforces more fluid in contact with solid MC surface. The enhancement in Nu is 60% and 50% compared to the plain MC case (MC). The dimple’s size has a significant effect on heat transfer performance because of increasing the flow recirculation after fluid leaves the dimples. The temperature along the MC for six cases at *Re* equals 200 is shown in Fig. 6. The surface of using (MC-FP-D1.0) significantly reduces the sink temperature by 7 compared to only using MC.

4.2. Effect of dimples and fillet profile on velocity, pressure drop and friction factor

The impact of dimples and the profile of the fillet on hydrodynamics characteristics of the microchannels is investigated. Different configurations include microchannels (MC), microchannels with fillet profile MC-FP, microchannels with dimples (MC-D) and microchannels with fillet profile, and microchannels with fillet and dimples (MC-FP-D) discussed. The contour of velocity distributions of MC surfaces is shown in Fig. 7 at *Re* is 1200 and ($z = 2$ mm). The dimples have a significant effect

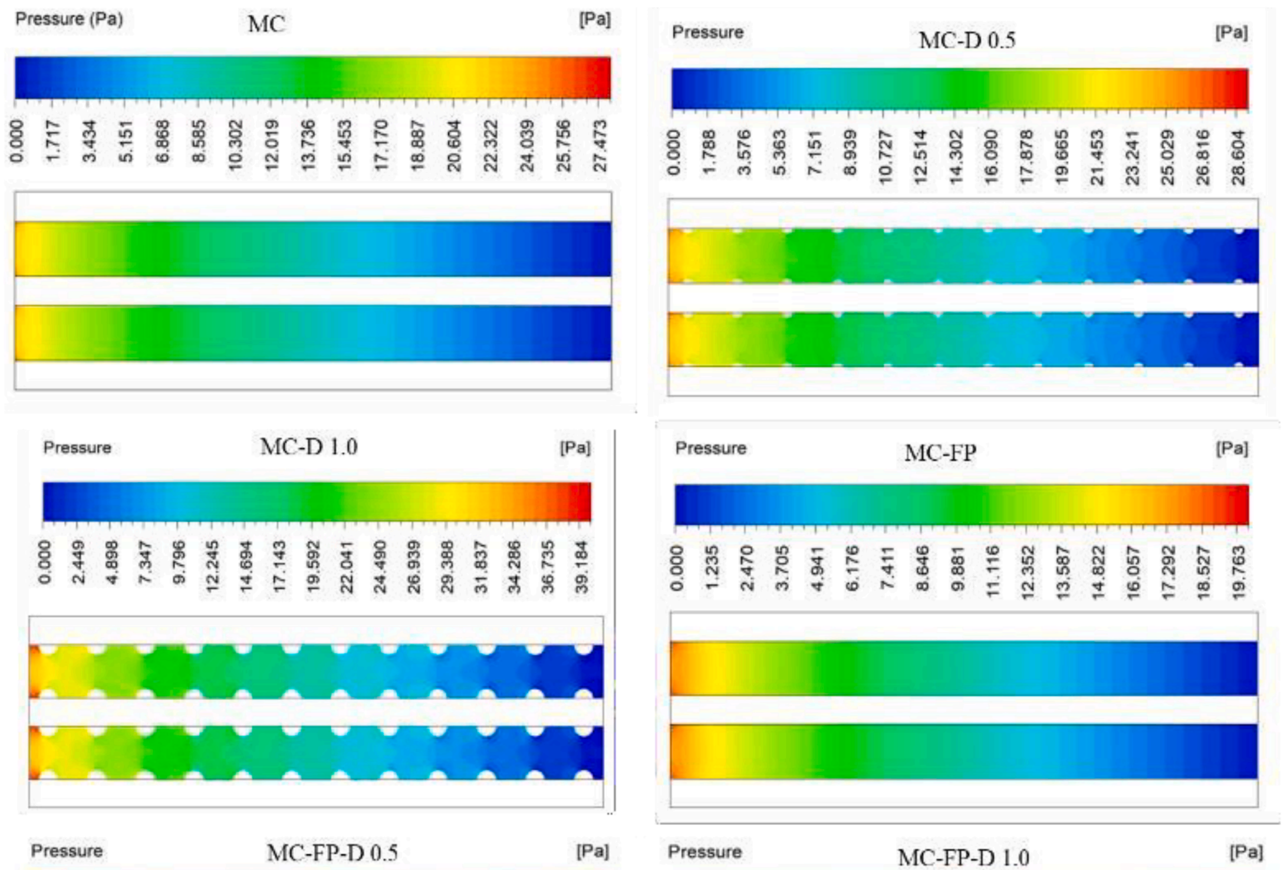

Fig. 8. The pressure distribution behaviours of modified MC in the x-y plane at (z = 2 mm) and Re = 200.

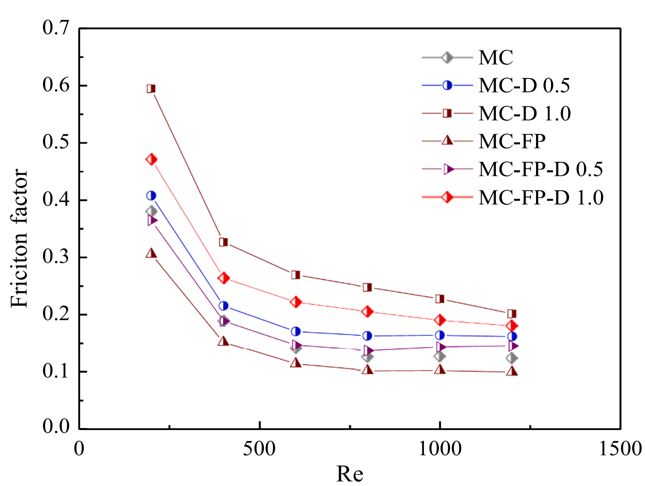

Fig. 9. The variation of friction losses at ranges of Re (200–1200).

Table 4
The (TPC) for all modified MCs.

Thermal performance criteria (TPC)					
Re	MC -D0.5	MC -D1.0	MC - FP	MC - FP- D0.5	MC - FP-D1.0
200	1.1013	0.7287	1.1204	1.0677	0.9506
600	1.1175	0.8049	1.5414	1.4541	1.35032
1000	1.1197	0.8967	1.5517	1.4569	1.34759

on fluid velocity distribution. The dimples size of 1 mm for MC increases the fluid velocity and circulation while the size of 0.5 mm reduces the fluid velocity. Dimples have the same behaviour of effect on fluid velocity in the fillet profile. Microchannels with a fillet profile and dimples have a lower fluid velocity than microchannels without a fillet profile and dimples. The dimples create mixing and circulation in fluid flow inside the channels as in cases (MC-D1.0) and (MC-FP-D1.0). The high fluid velocity is responsible increase the heat transfer performance.

Fig. 8 shows the pressure distribution of all configurations in the x-y plane at (z = 2 mm) and Re = 200. In the case of using dimples, the pressure drop lightly increases in comparison with the plain one. However, in the case of fillet profile, the pressure losses are lower than in cases of microchannels without fillet profile. By considering the influence of dimples and fillet profiles on pressure drop, a significant decrease of 30% in the case of MC-FP-D1.0 is less than in the case MC-D1.0. It can be noticed that the fillet profile not only enhances the thermal performance, but it reduces the pressure losses. This is obvious in Fig. 9 where friction losses are represented at ranges of Re (200–1200) for all case studies. The friction factor of the MC with dimples of 1 mm diameter gives the highest friction factor for all Re values. Dimple sizes have an impact on friction losses. At high Re, the variation in friction factor is small compared with friction factor at low Re values. In addition, the fillet profile eliminates the effect of friction losses. The friction factor of fillet microchannels with dimple sizes of 1 mm is 10% lower than microchannels with dimple sizes of 1 mm alone.

The thermal performance criteria were used to evaluate the MC's performance. TPC for all MCs that have been modified. The thermal performance criteria (TPC) for all cases are illustrated in Table 4. The calculations of TPC are obtained at different ranges of Reynolds number values. The results show that the TPC value increases with an increase in the Re values in modified surface cases. However, the dimples reduce the

TPC values because they increase the viscous forces and pressure losses which make MC-D1.0 the worst thermally performed one. Therefore, it is not recommended as the friction losses rise and dimple size should be minimized as shown in case MC-D0.5. The best TPC is obtained in fillet profile microchannels case MC – FP with and without dimples compared to other cases. An exemption is only at small *Re* which also gives a poor thermal performance. This is manipulated at intense flow. The optimal value is recorded at MC – FP for all *Re*. The high value of TPC tells the value of viscous forces is lower than the momentum forces. Fillet profile and dimples have a substantial impact on TPC values. Changing the dimple raises in size the value of TPC because it decreases the friction losses and viscous effect. The increase of Reynolds number increases the value of TPC in all cases of the microchannels.

5. Conclusions

In this study, the effect of dimples and fillet profile in microchannels has been systematically characterized in six cases through comparisons with the plain MC and between each other. The influence of dimple size on heat transfer performance is considered. Two dimple sizes were considered which are 0.5 mm and 1 mm. Dimples at various *Re* ranges have a significant impact on MC performance. The dimples increase the friction losses. In addition, the fillet profile MC provides better performance compared to and lower pressure drop losses than the plain MC. The dimples enhance the thermal performance with pressure drop penalties. The thermal performance criteria TPC are evaluated in all cases at different ranges of Reynolds number. The MC with fillet profile has the highest TPC value but it decreases with applying dimples. The dimples contribute to increasing the friction losses and lowering the TPC value.

Declaration of Competing Interest

The authors declare that they have no known competing financial interests or personal relationships that could have appeared to influence the work reported in this paper.

References

[1] R. Kempers, J. Colenbrander, W. Tan, R. Chen, A.J. Robinson, Experimental characterization of a hybrid impinging microjet-microchannel heat sink fabricated using high-volume metal additive manufacturing, Int. J. Thermofluids 5–6 (2020), 100029.
[2] Y.T. Yang, H. Sen Peng, Numerical study of thermal and hydraulic performance of compound heat sink, Numer. Heat Transf. A Appl. 55 (5) (2009) 432–447.
[3] M.Ebrahim Qomi, G.A. Sheikhzadeh, A. Fattahi, Heat transfer enhancement in a microchannel using a pulsating MHD hybrid nanofluid flow, Energy Sources, A Recover. Util. Environ. Eff. 00 (00) (2020) 1–16.
[4] F. Alnaimat, Heat transfer analysis of air-mist evaporative cooling in heat sink, Int. J. Thermofluids 14 (March) (2022), 100145.
[5] M.I. Hasan, H. Mohammed, G.A. Abid, Study of the axial heat conduction in parallel flow microchannel heat exchanger, J. King Saud Univ. - Eng. Sci. 26 (2) (2014) 122–131.
[6] H. Hasan, K. Egab, H. Hassan, Thermal and hydraulic characteristics study of different dimpled micro-channel heat sinks, AIP Conf. Proc. 2404 080009 (October) (2021).
[7] S.H. Menon, R. Rao A, J. Mathew, J. J, Derivation of Navier–Stokes equation in rotational frame for engineering flow analysis, Int. J. Thermofluids 11 (2021), 100096.
[8] K. Egab, S.K. Oudah, Thermal management analysis of li-ion battery-based on cooling system using dimples with air fins and perforated fins, Int. J. Therm. Sci. 171 (2021). July107200, 2022.
[9] Z. Alhajaj, A.M. Bayomy, M.Z. Saghir, M.M. Rahman, Flow of nanofluid and hybrid fluid in porous channels: experimental and numerical approach, Int. J. Thermofluids 1–2 (2020).
[10] M. Hajialibabaei, M.Z. Saghir, A critical review of the straight and wavy microchannel heat sink and the application in lithium-ion battery thermal management, Int. J. Thermofluids 14 (April) (2022), 100153.
[11] K. Egab, A. Okab, H.S. Dywan, S.K. Oudah, Enhancing a solar panel cooling system using an air heat sink with different fin configurations, in: IOP Conference Series: Materials Science and Engineering 671, 2020.
[12] W.D. Xu, et al., Study of two-phase flow distribution in microchannel heat exchanger header - a numerical simulation, Int. J. Thermofluids 14 (April) (2022), 100150.
[13] F. Alnaimat, Heat transfer analysis of air-mist evaporative cooling in heat sink, Int. J. Thermofluids 14 (January) (2022), 100145.
[14] P. Taylor, H. Kou, J. Lee, C. Lai, Thermal analysis and optimum fin length of a heat sink, Heat Transf. Eng. (April 2013) (2010) 37–41.
[15] W. Tang, L.C. Sun, H.T. Liu, M. Du, Improvements in performance of a self-similarity heat sink through structure modification, Heat Transf. Eng. 41 (17) (2020) 1512–1530.
[16] X. Yu, J. Feng, Q. Feng, Q. Wang, Development of a plate-pin fin heat sink and its performance comparisons with a plate fin heat sink, Appl. Therm. Eng. 25 (2–3) (2005) 173–182.
[17] O.N. Sara, T. Pekdemir, S. Yapici, M. Yilmaz, Heat-transfer enhancement in a channel flow with perforated rectangular blocks, Int. J. Heat Fluid Flow 22 (5) (2001) 509–518.
[18] C.-.W. Han, S.-.B. Jeong, Evaluation of the thermal performance with different fin shapes of the air-cooled heat sink for power electronic applications, J. Int. Counc. Electr. Eng. 6 (1) (2016) 17–25.
[19] S.K. Oudah, A. Tikadar, R. Fang, K. Egab, J.A. Khan, Thermohydraulic characteristics of a knurled microchannel heat sink in single phase regime, Therm. Fluids Eng. Conf. (2018) 1425–1436.
[20] S.K. Oudah, R. Fang, A. Tikadar, K. Egab, C. Li, J.A. Khan, The effects of hybrid sandblasting patterns on the heat transfer performance in a single-phase microchannel heat sink, in: ASME International Mechanical Engineering Congress and Exposition, Proceedings (IMECE) 8, 2017.
[21] S.K. Oudah, R. Fang, A. Tikadar, A.S. Salman, J.A. Khan, An experimental investigation of the effect of multiple inlet restrictors on the heat transfer and pressure drop in a flow boiling microchannel heat sink, Int. J. Heat Mass Transf. 153 (May) (2020), 119582.
[22] J. Ma, W. Li, C. Ren, J.A. Khan, C. Li, Realizing highly coordinated, rapid and sustainable nucleate boiling in micro-channelson HFE-7100, Int. J. Heat Mass Transf. 133 (2019) 1219–1229.
[23] W. Li, et al., Enhanced flow boiling in micro-channels using auxiliary channels and multiple micronozzles (I): characterizations of flow boiling heat transfer, Int. J. Heat Mass Transf. 116 (2018) 208–217.
[24] T. Alam, W. Li, W. Chang, F. Yang, J. Khan, C. Li, A comparative study of flow boiling HFE- 7100 in silicon nanowire and plainwall microchannels, Int. J. Heat Mass Transf. 124 (2018) 829–840.
[25] Z.S. Abdel-Rehim, Optimization and thermal performance assessment of pin-fin heat sinks, Energy Sources, A Recover. Util. Environ. Eff. 31 (1) (2009) 51–65.
[26] M.O. Qidwai, M.M. Hasan, N.Z. Khan, U. Khan, Optimization of heat transfer effects in radial fin microchannel heat sink, Energy Sources, A Recover. Util. Environ. Eff. 00 (00) (2019) 1–13.
[27] S.J. Kim, D.K. Kim, H.H. Oh, Comparison of fluid flow and thermal characteristics of plate-fin and pin-fin heat sinks subject to a parallel flow, Heat Transf. Eng. 29 (2) (2008) 169–177.
[28] A. Shadlaghani, M.R. Tavakoli, M. Farzaneh, M.R. Salimpour, Optimization of triangular fins with/without longitudinal perforate for thermal performance enhancement, J. Mech. Sci. Technol. 30 (4) (2016) 1903–1910.
[29] X. Hao, B. Peng, G. Xie, Y. Chen, Thermal analysis and experimental validation of laminar heat transfer and pressure drop in serpentine channel heat sinks for electronic cooling, J. Electron. Packag. Trans. ASME 136 (3) (2014).
[30] T. Izci, M. Koz, A. Koşar, The effect of micro pin-fin shape on thermal and hydraulic performance of micro pin-fin heat sinks, Heat Transf. Eng. 36 (17) (2015) 1447–1457.
[31] F. Ahmad, T.A. Cheema, M.M. Ur Rehman, A. Abbas, C.Woo Park, Thermal enhancement of microchannel heat sink using rib surface refinements, Numer. Heat Transf. A Appl. 76 (11) (2019) 851–870.
[32] A. Sakanova, Heat transfer enhancement of perforated pin heat sink in future aircraft applications, Appl. Therm. Eng. 124 (June) (2017) 315–326.
[33] K. Derakhshanpour, R. Kamali, M. Eslami, Effect of rib shape and fillet radius on thermal- hydrodynamic performance of microchannel heat sinks : a CFD study, Int. Commun. Heat Mass Transf. 119 (2020), 104928.
[34] G.I. Mahmood, P.M. Ligrani, Heat transfer in a dimpled channel: combined influences of aspect ratio, temperature ratio, Reynolds number, and flow structure, Int. J. Heat Mass Transf. 45 (10) (2002) 2011–2020.
[35] G. Lu, X. Zhai, Analysis on heat transfer and pressure drop of a microchannel heat sink with dimples and vortex generators, Int. J. Therm. Sci. 145 (2018), 105986. October2019.
[36] M.F. Ismail, M.N. Hasan, S.C. Saha, Numerical study of turbulent fluid flow and heat transfer in lateral perforated extended surfaces, Energy 64 (2014) 632–639.
[37] M.I. Hasan, Investigation of flow and heat transfer characteristics in micro pin fin heat sink with nanofluid, Appl. Therm. Eng. 63 (2) (2014) 598–607.
[38] A. Tikadar, T.C. Paul, S.K. Oudah, N.M. Abdulrazzaq, A.S. Salman, J.A. Khan, Enhancing thermal-hydraulic performance of counter flow mini-channel heat sinks utilizing secondary flow: numerical study with experimental validation, Int. Commun. Heat Mass Transf. 111 (2020), 104447.
[39] Kadhim Hakim T, et al., Numerical analysis of hybrid nanofluid natural convection in a wavy walled porous enclosure : local thermal non-equilibrium model, International Journal of Thermofluids (2022), https://doi.org/10.1016/j.ijft.2022.100190. In press.
[40] Ahmed Al-Manea, et al., Experimental and Numerical Study to Develop TRANSYS Model for an Active Flat Plate Solar Collector with an Internally Serpentine Tube Receiver, International Journal of Thermofluids 15 (2022) 100189, https://doi.org/10.1016/j.ijft.2022.100189.